

This article was downloaded by:

On: 23 January 2011

Access details: *Access Details: Free Access*

Publisher *Taylor & Francis*

Informa Ltd Registered in England and Wales Registered Number: 1072954 Registered office: Mortimer House, 37-41 Mortimer Street, London W1T 3JH, UK



## Journal of Coordination Chemistry

Publication details, including instructions for authors and subscription information:

<http://www.informaworld.com/smpp/title~content=t713455674>

### Catalytic activity of asymmetric monobenzoylmonobenzotetraazacyclo[14]tetradecinatonicel(II) complexes: X-ray crystal structure of monobenzo-2,4,9,11-tetramethyl-1,5,8,12-tetraazacyclo[14]tetradecinatonicel(II)

Dong Il Kim<sup>a</sup>; Eun Hee Kim<sup>a</sup>; Tapashi Ghosh Roy<sup>a</sup>; Hun Gil Na<sup>b</sup>; Zun Ung Bae<sup>a</sup>; Yu Chul Park<sup>a</sup>

<sup>a</sup> Department of Chemistry, Kyungpook National University, Daegu 702-701, Korea <sup>b</sup> Department of Chemistry, Daejin University, Pochon 487-800, Korea

**To cite this Article** Kim, Dong Il , Kim, Eun Hee , Roy, Tapashi Ghosh , Na, Hun Gil , Bae, Zun Ung and Park, Yu Chul(2005) 'Catalytic activity of asymmetric monobenzoylmonobenzotetraazacyclo[14]tetradecinatonicel(II) complexes: X-ray crystal structure of monobenzo-2,4,9,11-tetramethyl-1,5,8,12-tetraazacyclo[14]tetradecinatonicel(II)', *Journal of Coordination Chemistry*, 58: 3, 231 – 242

**To link to this Article:** DOI: 10.1080/00958970512331331334

**URL:** <http://dx.doi.org/10.1080/00958970512331331334>

PLEASE SCROLL DOWN FOR ARTICLE

Full terms and conditions of use: <http://www.informaworld.com/terms-and-conditions-of-access.pdf>

This article may be used for research, teaching and private study purposes. Any substantial or systematic reproduction, re-distribution, re-selling, loan or sub-licensing, systematic supply or distribution in any form to anyone is expressly forbidden.

The publisher does not give any warranty express or implied or make any representation that the contents will be complete or accurate or up to date. The accuracy of any instructions, formulae and drug doses should be independently verified with primary sources. The publisher shall not be liable for any loss, actions, claims, proceedings, demand or costs or damages whatsoever or howsoever caused arising directly or indirectly in connection with or arising out of the use of this material.

# Catalytic activity of asymmetric monobenzoylmonobenzo-tetraazacyclo[14]tetradecinatonicel(II) complexes: X-ray crystal structure of monobenzo-2,4,9,11-tetramethyl-1,5,8,12-tetraazacyclo[14]tetradecinatonicel(II)

DONG IL KIM<sup>†</sup>, EUN HEE KIM<sup>†</sup>, TAPASHI GHOSH ROY<sup>†</sup>,  
HUN GIL NA<sup>‡</sup>, ZUN UNG BAE<sup>†</sup> and YU CHUL PARK<sup>†\*</sup>

<sup>†</sup>Department of Chemistry, Kyungpook National University, Daegu 702-701, Korea

<sup>‡</sup>Department of Chemistry, Daejin University, Pochon 487-800, Korea

(Received 16 August 2004)

The complexes, 3-(*p*-Ymonobenzoyl)-Xmonobenzo-2,4,9,11-tetramethyl-1,5,8,12-tetraazacyclo[14]tetradecinato(2<sup>-</sup>)nickel(II), Y = CH<sub>3</sub>, H, Cl, NO<sub>2</sub> or OCH<sub>3</sub>, X = H (**A**) or NO<sub>2</sub> (**B**) have been synthesized and characterized. IR spectra of the complexes show intense bands in the region 1641–1647 cm<sup>-1</sup> attributed to the stretching modes of C=O. Electronic absorption spectra for the **A** series exhibit  $\pi \rightarrow \pi^*$  and ligand to metal charge transfer (LMCT) transitions, while for the **B** series an additional band appears between 440 and 452 nm, which might be due to another charge transfer. <sup>1</sup>H NMR spectra show an anisotropic magnetic effect due to the benzoyl group. Voltammograms of the complexes show two one-electron irreversible oxidation peaks in the range +100 to +800 mV and two, three or four reduction peaks between -1200 and -2800 mV, depending on substituents. Hammett plots of first and second oxidation potentials for the **A** series had slopes of 37 and 54 mV (22 and 39 mV for the **B** series), respectively. In oxidations of *p*-Zstyrenes (Z = OCH<sub>3</sub>, CH<sub>3</sub>, H, F or Cl) catalyzed by the complexes, conversion yields of substrates are appreciably affected by substituents of substrates and complexes. The structure of the precursor complex **1** with X = H and without any attached benzoyl group (orthorhombic, *P*2<sub>1</sub>2<sub>1</sub>2<sub>1</sub>, *a* = 7.923(6), *b* = 8.429(7), *c* = 24.18(2) Å, *Z* = 4, *R*1 = 0.0224 and *w*R2 = 0.0577) was characterized using single-crystal X-ray diffraction methods.

**Keywords:** Monobenzoylmonobenzotetraazacyclo[14]annulenenickel(II); LMCT and redox potential; X-Ray structure

## 1. Introduction

Tetraaza[14]annulene metal complexes have been widely investigated due to their structural features as model compounds of porphyrins and corrins in biological systems

\*Author for correspondence. Tel.: +82-53-950-5333. Fax: +82-53-950-6330. E-mail: ychpark@knu.ac.kr

and because of their catalytic activity [1–5]. Complexes reported include those with introduced functional groups such as *p*-substituted benzoyl chloride, nicotiny chloride, acetyl chloride, benzyl bromide, etc. on the periphery of the macrocyclic ring. However, most macrocyclic complexes are symmetrical, being disubstituted at methine sites, and examples of asymmetric complexes disubstituted at methine sites are few in number [6–11]. In a previous papers, we reported a series of asymmetric tetraaza[14 or 15]annulenenickel(II) complexes and investigated the effect of varying substituents such as CH<sub>3</sub>, Cl, NO<sub>2</sub> on the macrocyclic ring and of introducing the benzoyl group at the methine sites [12–15]. However, the effect of the incorporation of a benzene group on the chemical properties of these complexes has not been investigated in conjunction with those of a benzoyl group.

Herein, we report the synthesis of new asymmetrical tetraazaannulene 14- $\pi$  nickel(II) complexes with substituents (X = H or NO<sub>2</sub>) in the Xbenzene group and *p*-Ybenzoyl groups (Y = OCH<sub>3</sub>, CH<sub>3</sub>, H, Cl or NO<sub>2</sub>) at the methine site of the macrocycle ring by modifying a method described in the literature [13, 14]. These complexes were characterized using electronic, infrared, <sup>1</sup>H NMR and EI mass spectra. Redox potentials of the new complexes were measured using a glassy carbon electrode (GCE). Catalytic activities of the complexes were also investigated for oxidation of *p*-Zstyrene (Z = OCH<sub>3</sub>, CH<sub>3</sub>, H, F, Cl) in dichloromethane. The structure of the precursor complex **1** was investigated by X-ray diffraction analysis. This study provides information on the reactivity of the methine sites for synthesis of new complexes.

## 2. Experimental

### 2.1. Materials and measurements

Ni(OAc)<sub>2</sub>·4H<sub>2</sub>O, 1,2-Xphenylenediamine (X = H or NO<sub>2</sub>), *p*-Ybenzoylchloride (Y = CH<sub>3</sub>, H, Cl, NO<sub>2</sub> or OCH<sub>3</sub>), *p*-Zstyrene (Z = OCH<sub>3</sub>, CH<sub>3</sub>, H, F, Cl), ethylenediamine, 2,4-pentandione and triethylamine were purchased from Aldrich. Solvents CH<sub>3</sub>OH, CH<sub>2</sub>Cl<sub>2</sub> and C<sub>6</sub>H<sub>6</sub> were refluxed over calcium hydride under nitrogen, and checked for purity by GC just before use. Dimethylsulfoxide (DMSO) was purchased from Merck and used without further purification. Tetraethylammonium perchlorate (TEAP) used as supporting electrolyte was prepared and purified by the method described by Kolthoff and Coetzee [16]. Elemental analyses (C, H, N) of the complexes were carried out on a Carlo-Ebra EA 1108 instrument. Electronic absorption spectra were obtained on a Shimadzu UV-265 spectrophotometer. Infrared spectra were recorded on a Matteson Instruments Inc. Galaxy 7020 A spectrophotometer using KBr Pellets. <sup>1</sup>H NMR (300 MHz) spectra were recorded with a Bruker instrument using CDCl<sub>3</sub> with tetramethylsilane (TMS) as internal reference. EI mass spectra were determined with a JEOL MS-DX 300 gas chromatograph mass spectrometer at 70 eV using a direct inlet system.

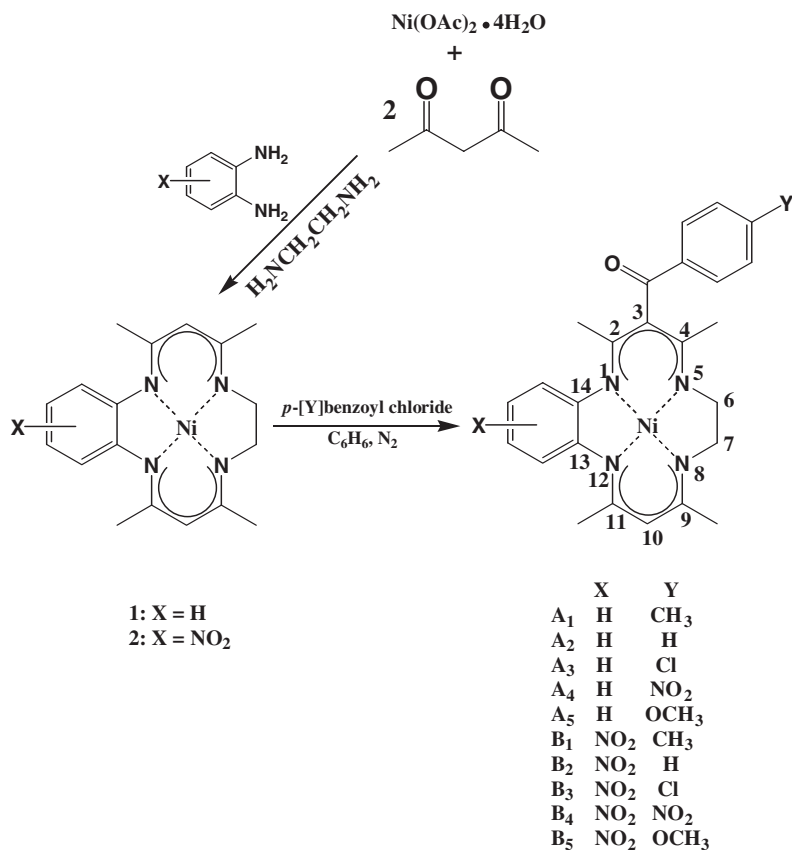
Cyclic voltammetry was performed using a Bioanalytical System (BAS) CV-50 W electrochemical analyzer and C2 cell stand at room temperature. The three electrode system for the electrochemical measurements was composed of a glassy carbon working electrode, an Ag/Ag<sup>+</sup> (0.01 M AgNO<sub>3</sub> in 0.1 M TEAP–DMSO solutions) reference electrode, and a platinum wire auxiliary electrode.

Analyses of organic products from oxidation reactions were made using a SHIMADZU GC-17A chromatographic system. The column temperature was programmed from 80 (5 min) to 100°C (15 min) at rate of 5°C min<sup>-1</sup>. Compounds were identified by comparison of retention times with those of pure compounds.

## 2.2. Synthesis

**2.2.1. 3-(*p*-Ybenzoyl)-Hmonobenzo-2,4,9,11-tetramethyl-1,5,8,12-tetraazacyclo[14]-tetradecinato(2-)-nickel(II) [Y = CH<sub>3</sub> (A<sub>1</sub>), H (A<sub>2</sub>), Cl (A<sub>3</sub>), NO<sub>2</sub> (A<sub>4</sub>), OCH<sub>3</sub> (A<sub>5</sub>)].** The complex **1** (0.001 mol, Scheme 1) prepared by a method reported in the literature [13–15] was dissolved in benzene (60 cm<sup>3</sup>) containing triethylamine (0.001 mol) and *p*-Ybenzoyl chloride (0.001 mol). The mixture was heated under reflux for 5 h with stirring and with bubbling nitrogen gas through the solution to protect it from moisture. In all syntheses, the reaction mixtures were left to stand at room temperature for 18 h and filtered to remove triethylamine hydrochloride. The filtrates were evaporated to dryness and resulting solids chromatographed on activated aluminium oxide and eluted with chloroform. The dark red products were obtained by recrystallizing from a 1:3 mixture of dichloromethane and methanol. For C<sub>26</sub>H<sub>28</sub>N<sub>4</sub>ONi (A<sub>1</sub>): Yield 43%. Anal. Calcd. (%): C, 66.27; H, 5.99; N, 11.89. Found: C, 66.11; H, 6.09; N, 11.87. IR (KBr disc, cm<sup>-1</sup>): ν(C=C), 1550; ν(C=N), 1631; ν(aromatic), 740 and 837; ν(C=O), 1641. UV-vis: λ<sub>max</sub>(nm) and ε<sub>max</sub>(M<sup>-1</sup> cm<sup>-1</sup>) in chloroform 375 and 33000, and 508 and 4050. EIMS: *m/z* 470 [M]<sup>+</sup>. For C<sub>25</sub>H<sub>26</sub>N<sub>4</sub>ONi (A<sub>2</sub>): Yield 45%. Anal. Calcd. (%): C, 65.67; H, 5.73; N, 12.26. Found: C, 65.87; H, 5.78; N, 11.97. IR (KBr disc, cm<sup>-1</sup>): ν(C=C), 1552; ν(C=N), 1631; ν(aromatic), 750 and 807; ν(C=O), 1641. UV-vis: λ<sub>max</sub> (nm) and ε<sub>max</sub> (M<sup>-1</sup> cm<sup>-1</sup>) in chloroform 376 and 28500, and 502 and 3700. EIMS: *m/z* 456 [M]<sup>+</sup>. For C<sub>25</sub>H<sub>25</sub>N<sub>4</sub>OClNi (A<sub>3</sub>): Yield 40%. Anal. Calcd. (%): C, 61.07; H, 5.13; N, 11.40. Found: C, 60.94; H, 5.39; N, 11.26. IR (KBr disc, cm<sup>-1</sup>): ν(C=C), 1549; ν(C=N), 1631; ν(aromatic), 753 and 852; ν(C=O), 1641. UV-vis: λ<sub>max</sub> (nm) and ε<sub>max</sub> (M<sup>-1</sup> cm<sup>-1</sup>) in chloroform 376 and 26000, and 498 and 3750. EIMS: *m/z* 490 [M]<sup>+</sup>. For C<sub>25</sub>H<sub>25</sub>N<sub>5</sub>O<sub>3</sub>Ni (A<sub>4</sub>): Yield 45%. Anal. Calcd. (%): C, 59.79; H, 5.02; N, 13.94. Found: C, 59.81; H, 5.24; N, 13.77. IR (KBr disc, cm<sup>-1</sup>): ν(C=C), 1558; ν(C=N), 1636; ν(aromatic), 745 and 849; ν(C=O), 1647; ν(NO<sub>2</sub>), 1340. UV-vis: λ<sub>max</sub> (nm) and ε<sub>max</sub> (M<sup>-1</sup> cm<sup>-1</sup>) in chloroform 372 and 26000, and 510 and 4900. EIMS: *m/z* 501 [M]<sup>+</sup>. For C<sub>26</sub>H<sub>28</sub>N<sub>4</sub>O<sub>2</sub>Ni (A<sub>5</sub>): Yield 40%. Anal. Calcd. (%): C, 64.09; H, 5.79; N, 11.50. Found: C, 63.83; H, 6.01; N, 11.26. IR (KBr disc, cm<sup>-1</sup>): ν(C=C), 1587; ν(C=N), 1637; ν(aromatic), 754 and 852; ν(C=O), 1647. UV-vis: λ<sub>max</sub> (nm) and ε<sub>max</sub> (M<sup>-1</sup> cm<sup>-1</sup>) in chloroform 376 and 27500, and 512 and 3350. EIMS: *m/z* 486 [M]<sup>+</sup>.

**2.2.2. 3-(*p*-Ybenzoyl)-NO<sub>2</sub>monobenzo-2,4,9,11-tetramethyl-1,5,8,12-tetraazacyclo[14]-tetradecinato(2-)-nickel(II) [Y = CH<sub>3</sub> (B<sub>1</sub>), H (B<sub>2</sub>), Cl (B<sub>3</sub>), NO<sub>2</sub> (B<sub>4</sub>), OCH<sub>3</sub> (B<sub>5</sub>)].** Complexes of the **B** series were prepared from a mixture of complex **2** (0.001 mol, scheme 1), triethylamine and *p*-Ybenzoyl chloride according to the procedure described above. The dark red products were obtained by recrystallizing from a 1:3 mixture of dichloromethane and methanol. For C<sub>26</sub>H<sub>27</sub>N<sub>5</sub>O<sub>3</sub>Ni (B<sub>1</sub>): Yield 10%. Anal. Calcd. (%): C, 60.49; H, 5.27; N, 13.57. Found: C, 60.23; H, 5.36; N, 13.33. IR (KBr disc, cm<sup>-1</sup>): ν(C=C), 1558; ν(C=N), 1636; ν(aromatic), 742 and 837; ν(C=O), 1642; ν(NO<sub>2</sub>), 1320. UV-vis: λ<sub>max</sub> (nm) and ε<sub>max</sub> (M<sup>-1</sup> cm<sup>-1</sup>) in chloroform 397 and 22000, 452 and 16500, and 522 and 12500. EIMS: *m/z* 515 [M]<sup>+</sup>.



Scheme 1.

For C<sub>25</sub>H<sub>25</sub>N<sub>5</sub>O<sub>3</sub>Ni (**B**<sub>2</sub>): Yield 4%. Anal. Calcd. (%): C, 59.79; H, 5.02; N, 13.94. Found: C, 59.53; H, 4.79; N, 13.73. IR (KBr disc, cm<sup>-1</sup>): ν(C=C), 1558; ν(C=N), 1633; ν(aromatic), 741 and 848; ν(C=O), 1641; ν(NO<sub>2</sub>), 1320. UV-vis: λ<sub>max</sub> (nm) and ε<sub>max</sub> (M<sup>-1</sup>cm<sup>-1</sup>) in chloroform 397 and 23600, 451 and 14200, and 517 and 11330. EIMS: *m/z* 501 [M]<sup>+</sup>. For C<sub>25</sub>H<sub>24</sub>N<sub>5</sub>O<sub>3</sub>ClNi (**B**<sub>3</sub>): Yield 7%. Anal. Calcd. (%): C, 55.95; H, 4.51; N, 13.04. Found: C, 55.92; H, 4.64; N, 12.72. IR (KBr disc, cm<sup>-1</sup>): ν(C=C), 1567; ν(C=N), 1631; ν(aromatic), 746 and 836; ν(C=O), 1641; ν(NO<sub>2</sub>), 1322. UV-vis: λ<sub>max</sub> (nm) and ε<sub>max</sub> (M<sup>-1</sup>cm<sup>-1</sup>) in chloroform 395 and 23900, 449 and 17900, and 519 and 11680. EIMS: *m/z* 535 [M]<sup>+</sup>. For C<sub>25</sub>H<sub>24</sub>N<sub>6</sub>O<sub>5</sub>Ni (**B**<sub>4</sub>): Yield 13%. Anal. Calcd. (%): C, 54.87; H, 4.42; N, 15.36. Found: C, 54.93; H, 4.63; N, 15.18. IR (KBr disc, cm<sup>-1</sup>): ν(C=C), 1562; ν(C=N), 1631; ν(aromatic), 726 and 851; ν(C=O), 1643; ν(NO<sub>2</sub>), 1320 and 1344. UV-vis: λ<sub>max</sub> (nm) and ε<sub>max</sub> (M<sup>-1</sup>cm<sup>-1</sup>) in chloroform 392 and 22500, 440 and 19000, and 526 and 12130. EIMS: *m/z* 546 [M]<sup>+</sup>. For C<sub>26</sub>H<sub>27</sub>N<sub>5</sub>O<sub>4</sub>Ni (**B**<sub>5</sub>): Yield 12%. Anal. Calcd. (%): C, 58.67; H, 5.11; N, 13.16. Found: C, 58.45; H, 5.31; N, 12.99. IR (KBr disc, cm<sup>-1</sup>): ν(C=C), 1571; ν(C=N), 1631; ν(aromatic), 744 and 850; ν(C=O), 1642; ν(NO<sub>2</sub>), 1319. UV-vis: λ<sub>max</sub> (nm) and ε<sub>max</sub> (M<sup>-1</sup>cm<sup>-1</sup>) in chloroform 397 and 25000, 452 and 17200, and 521 and 12620. EIMS: *m/z* 531 [M]<sup>+</sup>.

### 2.3. Catalytic oxidation of styrene derivatives

Catalytic oxidations were carried out in a 25 cm<sup>3</sup> round bottomed flask equipped with a side arm fitted with a screw-capped silicone septum. In a typical experiment, the complex (0.2 mmol) was put into a flask and then dichloromethane (4 cm<sup>3</sup>) was added, followed by a styrene derivative (2 mmol). After stirring for a few minutes, 10% NaClO solution (5 mmol) was injected, and the temperature was controlled at ambient. The reaction was monitored using GC by periodic sampling. The relative catalytic activities of the complexes as catalysts were simply considered using conversion yield (%) ( $100 \times [\text{final substrate}]/[\text{initial substrate}]$ ).

### 2.4. X-Ray crystallographic analysis

Preliminary examination and data collection for a crystal of complex **1** were performed with Mo K $\alpha$  radiation ( $\lambda = 0.71073 \text{ \AA}$ ) on an Enraf–Nonius CAD4 computer-controlled *k*-axis diffractometer equipped with a graphite crystal, incident-beam monochromator. Cell constants and orientation matrices for data collection were obtained from least-squares refinement of the setting angles of 25 reflections. The data were collected for Lorentz-polarization and absorption corrections were applied to the data. The structure was solved by direct methods using SHELXS-86 and refined by full-matrix least-squares calculations with SHELX-97 [17, 18]. The final cycle of the refinement converged with  $R1 = 0.0224$  and  $wR2 = 0.0577$ . Crystal data, details of the data collection and refinement parameters are listed in table 3. Selected bond distances and angles are presented in table 4.

## 3. Results and discussion

The asymmetric nickel(II) complexes with 14- $\pi$  monobenzoylated tetraazaannulene (**A** and **B** series) were prepared by procedures illustrated in Scheme 1. The condensation reaction between complex **1** (or **2**) and *p*-Ybenzoyl chloride in a 1:1 molar ratio in the presence of triethylamine was performed in refluxing benzene under a nitrogen atmosphere. Purification of the crude product was achieved by column chromatography on activated aluminium oxide and recrystallization from a mixture of dichloromethane and methanol. Data for elemental analyses, EI mass, infrared and electronic absorption spectra are given in the Experimental section, <sup>1</sup>H-nmr and cyclic voltammetry are collected in tables 1 and 2, respectively.

### 3.1. Spectroscopic properties

IR spectra of all complexes showed very intense bands in the region 1641–1647 cm<sup>-1</sup> attributed to the stretching modes of C=O, reflecting benzoylation at the methane site. This is supported by similar observations for nickel(II) complexes of asymmetric dibenzoylated tetraaza[14]annulenes [14]. The aromatic bands have two characteristic modes around 750 (macrocycle) and 850 cm<sup>-1</sup> (benzoyl group). The NO<sub>2</sub> of the benzoyl group and macrocycle exhibited strong bands at around 1340 and 1320 cm<sup>-1</sup>, respectively. C=C and C=N stretches occur around 1560 and 1630 cm<sup>-1</sup>, respectively, for all complexes.

Table 1.  $^1\text{H}$  NMR data for the asymmetric nickel(II) complexes.<sup>a</sup>

Comp.	Methyl	Methine	Ethylene	Y	Aromatic (macrocycle)	Aromatic (benzoyl)
<b>A<sub>1</sub></b>	2.289(s), 1.873(s)	5.076(s)	3.354(t)	2.418(s) (methyl)	6.702–7.208(m)	7.224(d)
	2.418(s), 2.090(s)		3.522(t)			7.800(d)
<b>A<sub>2</sub></b>	2.309(s), 1.867(s)	5.077(s)	3.334(t)		6.684–7.208(m)	7.411 ~ 7.912(m)
	2.418(s), 2.091(s)		3.530(t)			
<b>A<sub>3</sub></b>	2.310(s), 1.854(s)	5.078(s)	3.332(t)		6.688–7.204(m)	7.393(d)
	2.415(s), 2.090(s)		3.531(t)			7.818(d)
<b>A<sub>4</sub></b>	2.372(s), 1.832(s)	5.087(s)	3.339(t)		6.726–7.201(m)	7.979(d)
	2.417(s), 2.094(s)		3.558(t)			8.261(d)
<b>A<sub>5</sub></b>	2.283(s), 1.887(s)	5.076(s)	3.337(t)	3.875(s) (methoxy)	6.698–7.210(m)	6.907(d)
	2.420(s), 2.091(s)		3.521(t)			7.890(d)
<b>B<sub>1</sub></b>	2.132(s), 1.938(s)	5.265(s)	3.204(t)	2.422(s) (methyl)	7.150–7.294(m)	7.669(d)
	2.438(s), 2.282(s)		3.359(t)			7.834(d)
<b>B<sub>2</sub></b>	2.253(s), 1.922(s)	5.203(s)	3.392(t)		7.005–7.680(m)	7.915 ~ 8.117(m)
	2.494(s), 2.142(s)		3.575(t)			
<b>B<sub>3</sub></b>	2.307(s), 1.919(s)	5.269(s)	3.414(t)		7.150–7.692(m)	7.436(d)
	2.420(s), 2.134(s)		3.556(t)			7.855(d)
<b>B<sub>4</sub></b>	2.364(s), 1.888(s)	5.278(s)	3.421(t)		7.154–7.922(m)	8.023(d)
	2.422(s), 2.140(s)		3.600(t)			8.300(d)
<b>B<sub>5</sub></b>	2.285(s), 1.949(s)	5.265(s)	3.415(t)	3.897(s) (methoxy)	6.945–7.181(m)	7.921(d)
	2.422(s), 2.132(s)		3.548(t)			7.950(d)

<sup>a</sup>Chemical shifts in ppm from TMS as internal reference; measured in CDCl<sub>3</sub> at 300 MHz; multiplicity of a proton signal is given in parentheses after  $\delta$  value; s = singlet, d = doublet, t = triplet, m = multiplet.

Table 2. Redox potential data for the asymmetric nickel(II) complexes.<sup>a</sup>

Comp.	Ep(1), mV	Ep(2), mV	En(L), mV	En(m), mV
<b>A<sub>1</sub></b>	+170	+717	–2342	–2642
<b>A<sub>2</sub></b>	+175	+727	–2276	–2646
<b>A<sub>3</sub></b>	+187	+742	–2081, –2272	–2676
<b>A<sub>4</sub></b>	+203	+760	–1229, –1759	–2707
<b>A<sub>5</sub></b>	+164	+698	–2402	–2694
<b>B<sub>1</sub></b>	+337	+678	–1563, –2250, –2407	–2759
<b>B<sub>2</sub></b>	+331	+682	–1555, –2211, –2381	–2772
<b>B<sub>3</sub></b>	+353	+708	–1559, –2116, –2350	–2768
<b>B<sub>4</sub></b>	+350	+700	–1194, –1585, –1772, –2333	–2767
<b>B<sub>5</sub></b>	+327	+653	–1563, –2246, –2459	–2772

<sup>a</sup>All data were measured in 0.1 M TEAP–DMSO solution vs. Ag/Ag<sup>+</sup> (0.01 M AgNO<sub>3</sub> in DMSO) at 25°C.

Electronic absorption spectra of the complexes showed two absorption bands between 370 and 530 nm. The complexes (**B** series) with an NO<sub>2</sub> group exhibited an additional band between 440 and 452 nm which may be accounted for by charge transfer. The bands in the near UV region (370–400 nm) with molar absorptivities of 14000 to 34000 M<sup>-1</sup> cm<sup>-1</sup> are attributed to  $\pi \rightarrow \pi^*$  transitions. Spectra in the visible region showed bands at 498–526 nm ( $\epsilon_{\text{max}} = 3000\text{--}13000\text{ M}^{-1}\text{ cm}^{-1}$ ) attributed to ligand to metal charge transfer (LMCT) from the highest occupied ligand molecular orbital to the lowest empty d-orbital of nickel. The maxima of LMCT transitions for the complexes were at longer wavelengths than those without the benzoyl group, but lower than those with dibenzoyl groups. This could be explained by the notion that benzoylation increases interaction between nickel(II) and nitrogen atoms of the macrocycle ring by an expanded  $\pi$ -conjugation system in the macrocycle ring.

Table 3. Crystal data and structure refinement details for complex 1.

Empirical formula	C <sub>18</sub> H <sub>20</sub> N <sub>4</sub> Ni
Formula weight	351.09
Temperature/K	173(2)
Wavelength/Å	0.71073
Crystal system	Orthorhombic
Space group	<i>P</i> 2 <sub>1</sub> 2 <sub>1</sub> 2 <sub>1</sub>
Unit cell dimensions/Å, °	<i>a</i> = 7.923(6) α = 90 <i>b</i> = 8.429(7) β = 90 <i>c</i> = 24.18(2) γ = 90
Volume/Å <sup>3</sup>	1615(2)
<i>Z</i>	4
Density (calculated)/Mg m <sup>-3</sup>	1.444
Absorption coefficient/mm <sup>-1</sup>	1.206
<i>F</i> (000)	736
Crystal size/mm <sup>3</sup>	0.62 × 0.38 × 0.25
Theta range for data collection/°	1.68 to 28.25
Index ranges	-10 ≤ <i>h</i> ≤ 10 -11 ≤ <i>k</i> ≤ 10 -31 ≤ <i>l</i> ≤ 31
Reflections collected	9601
Independent reflections	3751 ( <i>R</i> (int) = 0.0142)
Completeness to theta = 28.25° (%)	97.1
Absorption correction	Semi-empirical from equivalents
Max., min. transmission	0.7526, 0.5219
Refinement method	Full-matrix least-squares on <i>F</i> <sup>2</sup>
Data/restraints/parameters	3751/0/288
Goodness-of-fit on <i>F</i> <sup>2</sup>	1.091
Final <i>R</i> indices [ <i>I</i> > 2σ( <i>I</i> )]	<i>R</i> 1 = 0.0224, <i>wR</i> 2 = 0.0577
<i>R</i> indices (all data)	<i>R</i> 1 = 0.0233, <i>wR</i> 2 = 0.0582
Absolute structure parameter	0.027(11)
Largest diff. peak and hole/e Å <sup>-3</sup>	0.336 and -0.262

Table 4. Selected bond distances (Å) and angles (°) for complex 1.

Ni(1)–N(1)	1.8726(17)	Ni(1)–N(2)	1.8732(18)
Ni(1)–N(3)	1.8645(18)	Ni(1)–N(4)	1.8610(18)
N(1)–C(1)	1.412(2)	N(1)–C(17)	1.348(2)
N(2)–C(6)	1.411(2)	N(2)–C(7)	1.349(2)
N(3)–C(10)	1.315(3)	N(3)–C(12)	1.458(3)
N(4)–C(13)	1.456(3)	N(4)–C(14)	1.318(3)
C(1)–C(2)	1.400(3)	C(1)–C(6)	1.420(3)
C(7)–C(8)	1.514(3)	C(7)–C(9)	1.389(3)
C(9)–C(10)	1.401(3)	C(9)–C(11)	1.507(3)
C(12)–C(13)	1.409(4)		
N(1)–Ni(1)–N(2)	85.60(7)	N(4)–Ni(1)–N(1)	94.03(8)
N(4)–Ni(1)–N(3)	85.84(8)	N(4)–Ni(1)–N(2)	179.00(7)
N(3)–Ni(1)–N(1)	179.03(7)	N(3)–Ni(1)–N(2)	94.52(8)
C(10)–N(3)–C(12)	119.86(18)	C(7)–N(2)–C(6)	124.39(15)
C(10)–N(3)–Ni(1)	126.21(13)	C(7)–N(2)–Ni(1)	123.72(13)
C(12)–N(3)–Ni(1)	113.35(14)	C(6)–N(2)–Ni(1)	111.46(11)
N(2)–C(6)–C(1)	113.56(14)	N(2)–C(7)–C(8)	122.75(17)
N(2)–C(7)–C(9)	121.64(16)	N(3)–C(10)–C(9)	121.53(17)
C(7)–C(9)–C(10)	126.96(17)	N(3)–C(10)–C(11)	121.35(19)
C(8)–C(7)–C(9)	115.60(16)	C(13)–C(12)–N(3)	111.9(2)
C(9)–C(10)–C(11)	117.12(18)		



Chemical shifts in  $^1\text{H}$  NMR spectra and assignments are listed in table 1, based on comparisons with complexes reported earlier [12–15]. Resonances for the 2- and 4-methyl groups move upfield (0.2–0.4 ppm) compared to 9- and 11-methyl groups [19]. This observation reflects that fact that the methyl groups are subject to a shielding effect caused by the magnetic anisotropy of the benzoyl group lying out of the plane of the macrocyclic ring. Resonances for the ethylene protons appear as two triplets because of the benzoyl group. The methine proton peak opposite the benzoyl group is little affected by the substituents.

### 3.2. Electrochemical behavior and Hammett plots

Redox potentials of the complexes measured in 0.1 M TEAP–DMSO solutions vs  $\text{Ag}/\text{Ag}^+$  (0.01 M) at sweep rate of  $100\text{ mV s}^{-1}$  and  $25^\circ\text{C}$  are collected in table 2. Typical voltammograms in the range  $+1100$  to  $-3000\text{ mV}$  vs  $\text{Ag}/\text{Ag}^+$  are illustrated in figure 1. The cyclic voltammograms of the **A** and **B** series show two irreversible oxidation waves in the range  $+100$  to  $+800\text{ mV}$  and two to four reduction waves in the range  $-1200$ – $2700\text{ mV}$ , depending on substituents, respectively. Asymmetric tetraaza[14] annulene nickel(II) complexes without a benzoyl group show only a reduction peak ( $\text{Ni}^{2+} \rightarrow \text{Ni}^+$ ) at around  $-2600\text{ mV}$  [15]. The reduction peaks must be also associated

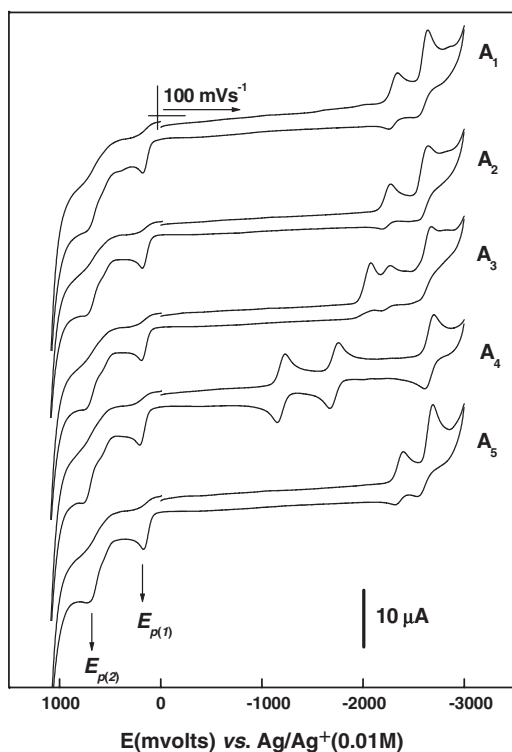


Figure 1. Cyclic voltammograms of the **A** series complexes (0.001 M) in 0.1 M TEAP–DMSO solutions vs  $\text{Ag}/\text{Ag}^+$  (0.01 M) at  $25^\circ\text{C}$  and scan rate of  $100\text{ mV s}^{-1}$ .

with both the benzoyl group and its substituents. The substituent effect of the benzoyl group on the potentials was examined by means of a Hammett plot (figure 2) using substituent constant  $\sigma_p$  values [20]. The relationships between  $E_p$  (V) and  $\sigma_p$  for the first and the second oxidation peaks of the **A** series were linear with positive slopes of +37 and +54 mV (+22 and +39 mV for the **B** series). These slopes are similar to results involving oxidation potentials for metalloporphyrins with  $\beta$ -substituents located on the pyrrole residues of the porphyrin ligand [21, 22]. The substituent effect on the potential was not large, but clearly defined. However, an electronic effect on the reduction wave due to  $\text{Ni}^{2+} \rightarrow \text{Ni}^+$  at around  $-2700$  mV could not definitely be determined.

### 3.3. Catalytic oxidation of styrene derivatives

Simple results for catalytic oxidations of several styrene derivatives are illustrated in figure 3. The **B** series complexes with an electron withdrawing group ( $\text{NO}_2$ ) on the macrocycle ring, inducing a lower electron density on the metal center, generally show somewhat higher activities than the **A** series. This could be explained in terms of varying electron density at the metal, affecting the formation of activated metal–olefin complexes [23]. Depending on the substituents in the complexes, the conversion % of substrates increased in the order  $p\text{-OCH}_3$  ( $-0.27$ ) <  $p\text{-CH}_3$  ( $-0.17$ ) <  $\text{H}$  ( $0$ ) <  $p\text{-Cl}$  ( $+0.23$ ) <  $p\text{-NO}_2$  ( $+0.78$ ). The order agrees with the  $\sigma_p$  values (parenthesized). On the other hand, the substituent effects on styrene on the conversion % of substrates (figure 4) were opposite to those of the complexes (figure 3). An electron withdrawing

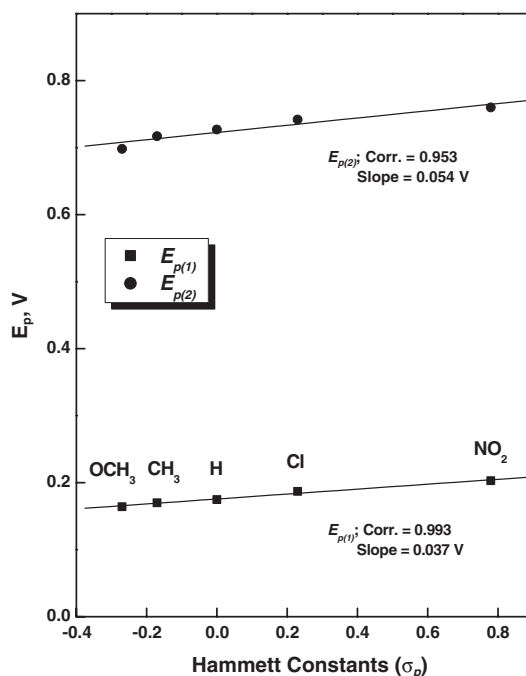


Figure 2. Hammett plots of first and second oxidation potentials vs  $\text{Ag}/\text{Ag}^+$  (0.01 M) in 0.1 M TEAP–DMSO as a function of substituent constants for the **A** series complexes (0.001 M) at  $25^\circ\text{C}$  and scan rate of  $100\text{ mV s}^{-1}$ .

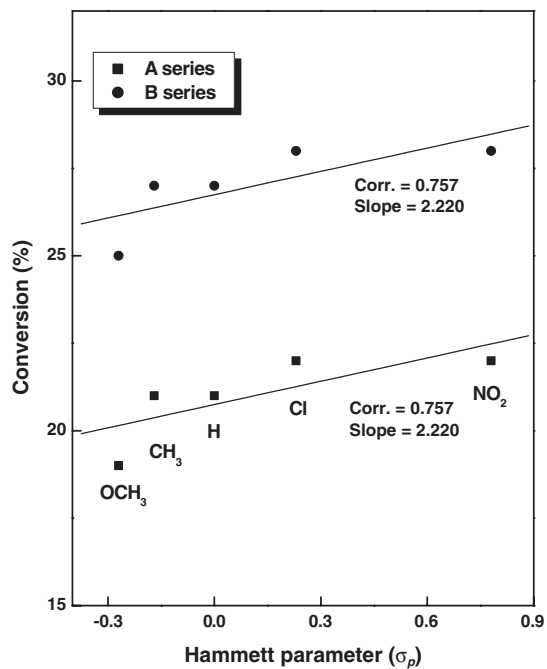


Figure 3. Hammett plots of substrate conversion (%) vs  $\sigma_p$  values for oxidation of styrene derivatives catalyzed by the complexes **A** series and **B** series at room temperature.

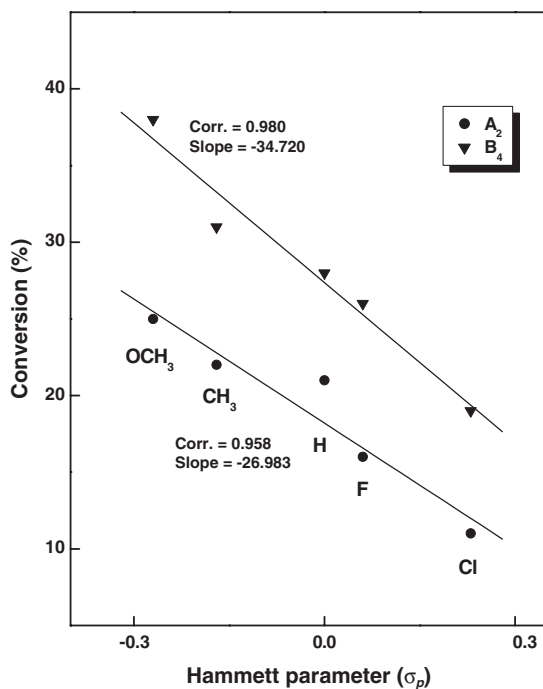


Figure 4. Hammett plots of conversion (%) vs  $\sigma_p$  values of *p*-[Z]styrene for **A**<sub>2</sub> and **B**<sub>4</sub>.

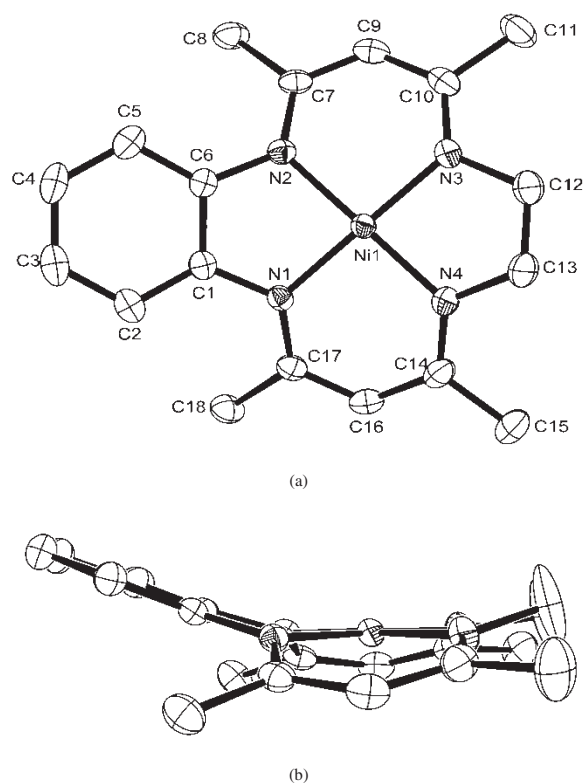


Figure 5. The X-ray structure showing the atom numbering scheme (a) and side view (b) of monobenzoyl-2,4,9,11-tetramethyl-1,5,8,12-tetraazacyclo[14]tetradecinato(2<sup>-</sup>)nickel(II).

group on styrene decreases the  $\pi$  electron density of styrene as a nucleophile, making it more difficult to attack an electrophilic metal center. Therefore, the substituent effect on the catalytic oxidation of styrenes involves both variance of electron density at the metal center and the olefin double bond.

### 3.4. X-Ray structure

The molecular structure of complex **1** is shown in figure 5. The average bond distance (1.8628 Å) for Ni(1)–N(1) and Ni(1)–N(2) is longer than that (1.8729 Å) of Ni(1)–N(3) and Ni(1)–N(4) attributable to differences in basicities of phenylenediamine ( $pK_{a1}$  and  $pK_{a2}$ , 1.81 and 4.61) and ethylenediamine ( $pK_{a1}$  and  $pK_{a2}$ , 7.08 and 9.89) [24]. The N–C distances in the six-membered rings are 1.348 for N(1)–C(17), 1.349 for N(2)–C(7), 1.315 for N(3)–C(10) and 1.318 Å for N(4)–C(14), while for five-membered rings they are longer (1.412 for N(1)–C(1), 1.411 for N(2)–C(6), 1.458 for N(3)–C(12) and 1.456 Å for N(4)–C(13)). The average C–C distance in the six-membered chelate rings is 1.395 Å close to that of benzene (1.40 Å), reflecting the aromaticity of the macrocycle ring. The average N–Ni–N angles of five- and six-membered rings are 85.72 and 94.28°, respectively, and N(3)–Ni(1)–N(1) and N(4)–Ni(1)–N(2) are 179.03 and 179.00°, respectively, indicating the geometry

involving nickel and the four nitrogen atoms is slightly distorted square planar. The structure shows a saddle shape, similar to that of the symmetric dibenzotetraazacyclo[14]annulene nickel(II) complex.

### Supplementary material

Crystallographic data for the structural analysis have been deposited at the CCDC, 12 Union Road, Cambridge CB2 1EZ, UK on request, quoting the deposition number CCDC 245071. Copies of this information can be obtained free of charge via E-mail: deposit@ccdc.cam.ac.uk or www: <http://www.ccdc.cam.ac.uk>; Tel: +44-1233-336031; Fax: +44-1223-336033.

### Acknowledgments

This work was supported by a Korea Research Foundation Grant (KRF-2004-005-C00009).

### References

- [1] R.D. Bereman, M.R. Churchill, G.D. Shields. *Inorg. Chem.* **18**, 3117 (1979).
- [2] R.D. Bereman, G.D. Shields, J. Bordner, J.R. Dorfman. *Inorg. Chem.* **20**, 2165 (1981).
- [3] C.L. Bailey, R.D. Bereman, D.P. Rillema, R. Nowak. *Inorg. Chem.* **23**, 3956 (1984).
- [4] M.C. Weiss, G.C. Gordon, V.L. Goedken. *Inorg. Chem.* **18**, 758 (1979).
- [5] C.L. Bailey, R.D. Bereman, D.P. Rillema, R. Nowak. *Inorg. Chem.* **25**, 933 (1986).
- [6] K. Sakata, K. Koyanagi, M. Hashimoto. *J. Heterocyclic Chem.* **32**, 329 (1995).
- [7] K. Sakata, M. Itoh. *J. Heterocyclic Chem.* **29**, 921 (1992).
- [8] J.C. Dabrowiak, D. Fisher, F.C. McElroy, D.J. Macero. *Inorg. Chem.* **18**, 2304 (1979).
- [9] K. Sakata, M. Hashimoto, T. Hamada, S. Matsuno. *Polyhedron* **15**, 967 (1996).
- [10] E.M. Opozda, W. Lasocha. *Inorg. Chem. Commun.* **3**, 239 (2000).
- [11] J. Eilmes. *Polyhedron* **4**, 943 (1985).
- [12] Y.C. Park, Z.U. Bae, S.S. Kim, S.K. Baek. *Bull. Korean Chem. Soc.* **16**, 287 (1995).
- [13] Y.C. Park, S. S. Kim, H.G. Na, Y.I. Noh. *J. Coord. Chem.* **41**, 191 (1997).
- [14] Y.C. Park, H.G. Na, J.H. Choi, J.C. Byun, E.H. Kim, D.I. Kim. *J. Coord. Chem.* **55**, 505 (2002).
- [15] Y.C. Park, S.S. Kim, D.C. Lee, C.H. An. *Polyhedron* **16**, 253 (1997).
- [16] I.M. Kolthoff, J.F. Coetzee. *J. Am. Chem. Soc.* **79**, 1852 (1957).
- [17] G.M. Sheldrick. *Acta Crystallogr., Sect. A* **46**, 467 (1990).
- [18] G.M. Sheldrick. SHELX-97, University of Göttingen, Germany (1997).
- [19] K. Sakata, H. Tagami, M. Hashimoto. *J. Heterocyclic Chem.* **26**, 805 (1995).
- [20] N. Issaacs. *Physical Organic Chemistry* 2nd edn. (Longman Scientific & Technical, London 1995), pp. 146–192.
- [21] A. Giraudeau, H.J. Callot, M. Gross. *Inorg. Chem.* **18**, 201 (1979).
- [22] A. Giraudeau, H.J. Callot, J. Jordon, I. Ezhar, M. Gross. *J. Am. Chem. Soc.* **101**, 3857 (1979).
- [23] R. Sinigaglia, R.A. Michelin, F. Pinna, G. Strukul. *Organometallics* **6**, 728 (1987).
- [24] A. Mederos, A. Dominguez, R.H. Molina, J. Sanchiz, R. Brito. *Coord. Chem. Rev.* **193–195**, 913 (1999).